Green's-function diagrammatic technique for complicated level systems. II. An application to the spin-1 Heisenberg ferromagnet with easy-axis single-ion anisotropy*

David Hsing-Yen Yang and Yung-Li Wang
Department of Physics, Florida State University, Tallahassee, Florida 32306
(Received 3 March 1975)

The Green's-function diagrammatic expansion technique developed by the authors is applied to a spin-1 Heisenberg ferromagnet with easy-axis single-ion anisotropy. Inconsistency, which prevails in the previous random-phase-approximation equation-of-motion calculations, is examined and shown to be eliminated in the present calculation. Spin-wave energies, correlation functions, and magnetization are calculated to the zeroth order and first order in $1/z$. Critical temperature is determined (in fact, for a more general system which includes also the anisotropic exchange interaction) and compared with the values obtained by the high-temperature-expansion technique. The agreement is generally within a few percent (less than 1% for the Ising cases). At low temperatures, the second order in $1/z$ calculation is carried out. We show, in the temperature expansion of the magnetization, Dyson's T^4 correction to the first Born approximation, along with a series of terms led by $T^2e^{-\beta D}$ due to the single-ion anisotropy.

I. INTRODUCTION

The Green's-function approach to the spin-1 Heisenberg ferromagnetic system with an easy-axis single-ion anisotropy has been a subject of interest in recent years. The reason is quite obvious. First of all, the single-ion anisotropy prevails in almost all magnetic crystals, its effects are thus of prime interest. For a spin-1 system, the single-ion anisotropy is of second order in the spin variables, and becomes further simplified if the system has a uniaxial symmetry. Thus, the spin-1 uniaxial ferromagnet provides a simple system for the theoretical investigation using the Green's-function technique which has been proved successful in treating the simpler isotropic Heisenberg systems.

In general, there are two ways to calculate the Green's functions: the equation-of-motion technique and the diagrammatic expansion method. Double-time temperature-dependent Green's functions are generally employed in the equation-of-motion technique. The higher-order Green's functions are decoupled often with the random-phase approximation (RPA) because it is simple to apply and conforms to the intuitive effective-field picture. For ferromagnets with a single-ion anisotropy some complications arise. Initially, the decoupling of the Green's functions generated from the anisotropy terms presented some difficulties because it would require breaking up a product of operators of the same site in the Green's functions. Lines[1] has devised a rather complicated scheme to cope with the situation. The scheme is nevertheless valid only in the weak-anisotropy limit. Actually, there is no need to decouple the Green's functions generated from the anisotropy term. Unlike the exchange interaction, being a single-ion potential, the anisotropy potential does not transfer excitations from one site to another. Consequently, the Green's functions generated from the anisotropy would all have the same site indices and under commutation they eventually close the chain. Indeed, for spin 1, as shown first by Murao and Matsubara,[2] it is sufficient to decouple the Green's functions generated by the exchange potential in the RPA. The Green's functions $\langle\langle S^+; B\rangle\rangle$ and $\langle\langle S^+S^z + S^zS^+; B\rangle\rangle$ would then couple to each other, and only to each other, in the equations of motion. In this way the anisotropy can be accounted for exactly, and the results are expected to be valid for the whole range of anisotropy strength.

However, a new question was raised. It was noted by Murao and Matsubara[2] that for spin 1, there are three dipolar and five quadrupolar operators, which form a complete set along with the unity operator. From these operators various Green's functions can be constructed. A physical quantity, such as magnetization, can usually be obtained from more than one of these Green's functions. The fact that generally they do not yield consistent results makes the selection of Green's function, or a set of Green's functions when they are coupled together, for the calculation of magnetization, e.g., an essential problem. While the source of inconsistency lies clearly in the decoupling approximation, there is no simple remedy available. This lack of consistency in the determination of a correlation function from the Green's functions was called "redundancy" by Murao and Matsubara. These authors, however, went on and chose a set of Green's functions, mostly based on their intuition, to carry out the calculations. In later works, Devlin,[3] Tanaka and Kondo,[4] and Potapkov[5] have avoided the redundancy ostensibly. Their treatment consists of using the set of Green's functions

which would, in the zero-anisotropy limit, yield the familiar RPA results of the isotropic Heisenberg ferromagnet. Haley and Erdös[6] used a different formalism. They constructed the Green's functions from the "standard-basis operators" as was also proposed by Hubbard[7] as the atomic representation formulation in a tight-band-model calculation. The idea is to use the eigenstates of the single-ion effective Hamiltonian as the basis for the calculation. The standard-basis operators which annihilate an ion in one basis state and, simultaneously, create the ion in another (or the same) state are defined and the original Hamiltonian is then projected onto this manifold. In this formalism the source of the inconsistency becomes even more explicit. As a way to recover the existing RPA results of the isotropic Heisenberg ferromagnet, Haley and Erdös suggested to "enforce" externally the kinematic restriction, which forbids more than one energy level of a single ion be occupied, by setting to zero the corresponding autocorrelation functions in the calculation. Their procedure can be shown to be equivalent to the selection of a particular set of Green's functions, and in fact, the same set as used in Refs. 3–5. The method of Haley and Erdös has been applied to an antiferromagnetic system with single-ion anisotropy by Vettier.[8] Recently, to cope with the problem of redundancy, Egami and Brooks[9] have proposed a scheme for the evaluation of the magnetization with part of the kinematic restriction included in the calculations. Their results would agree with the results of Haley and Erdös had the latter authors not enforced the kinematic restriction by setting the corresponding autocorrelation functions to zero in their calculations. As in the other RPA theories, the theory of Egami and Brooks also fails to reproduce the correct low-temperature behavior. Furthermore, an unphysical term appears in their theory, and, if not set to zero, would lead to erroneous results when $D/J(0)$ is large. As discussed by Egami and Brooks, these difficulties are inherent in the decoupling theories.

While the inconsistency persists as a result of the decoupling approximation in the equation-of-motion method, it can be eliminated entirely in the calculation using the diagrammatic expansion technique which has been applied to some simple systems[10,11] successfully. The problem of the easy-axis ferromagnet with a single-ion anisotropy has also been attacked by several authors. In the work of Matlak[12] and of Matlak and Westwanski[13] the anisotropy potential was treated as a part of the interaction Hamiltonian. The diagrams become rather complicated. Apparently unaware of the inconsistency in the RPA theory, they strived to get the same results. Kaschenko *et al.*,[14] on the other hand, included the anisotropy potential in the unperturbed Hamiltonian. But, the "time" (temperature) behavior of the spin operators in the interaction picture becomes too complicated to allow for a tractable Wick-like theorem for the spin operators and they were forced to calculate the ordered products directly.

Very recently we have developed a Green's-function diagrammatic technique using the standard-basis operators[15] (hereafter referred to as I). The method makes possible a Green's-function calculation of systems with complicated energy-level structures. In this paper we apply the technique developed in I to the spin-1 uniaxial ferromagnetic system with single-ion anisotropy. The easy-axis case is considered here; the hard-axis case will be given in a later publication. Although the single-ion anisotropy potential is included in the unperturbed Hamiltonian, the time behaviors of the standard-basis operators still assume simple forms. The calculation is self-consistent in all respects; the sum rules and the kinematic conditions are preserved. The diagrams are classified *formally* in the orders of powers of $1/z$, z being the effective number of spin interacting with a given spin. Also known as the high-density expansion,[16] the series gives the molecular-field-theory result in the zeroth order. The first-order correction is obtained by summing all single-loop diagrams in which *one* free-momentum variable is summed over. The higher-order corrections are similarly defined, and self-consistency is preserved in each order.

In Sec. II the diagrammatic expansion technique applied to the present system, as a special case of the general theory developed in I, is briefly reviewed. Calculations of Green's functions and correlation functions to the zeroth order in $1/z$ are given in Sec. III. The inconsistency involved in the RPA equation-of-motion calculation is also discussed. First-order corrections are given in Sec. IV. The spin-wave energy shift is obtained. Considering a correlation function as an example, we show the preservation of kinematics of the spin operators in the diagrammatic calculation. In Sec. V we consider the thermodynamics of the system. We first calculate the populations of the three basis molecular-field levels to the first-order approximation by summing all single-loop diagrams. All single-ion quantities are then obtainable as linear combinations of the three populations. The Curie temperature is calculated. In the calculation of the Curie temperature we have made a simple but important generalization to include the case of anisotropic exchange interaction. Results are compared with the values obtained in the high-temperature-expansion calculation. At low temperatures the first-order approximation reduces to the usual spin-wave approximation which ignores spin-wave interactions. We thus carry out the calculation to

the second order, summing diagrams with two loops. We show in the isotropic case, as also obtained by Vaks, Larkin, and Pikin,[10] the Dyson's T^4 correction to the magnetization in the first Born approximation and the absence of the T^3 term erroneously predicted by the RPA theory. For the anisotropic ferromagnet, a series of terms with the leading-order term proportional to $T^2e^{-\beta D}$ are obtained along with the Dyson's correction.

II. DIAGRAMMATIC EXPANSION

The Hamiltonian of the system can be written as

$$\mathcal{H} = -\sum_{i,j} J_{ij}(S_i^z S_j^z + S_i^+ S_j^-) - D\sum_i (S_i^z)^2 - g\mu_B H\sum_i S_i^z , \tag{2.1}$$

where $S=1$, $D>0$, and H is the external magnetic field applied along the anisotropy axis. We separate the Hamiltonian into two parts:

$$\mathcal{H} = \mathcal{H}_0 + \mathcal{H}_{\text{int}} , \tag{2.2}$$

where $\mathcal{H}_0$ is the single-ion effective-field Hamiltonian which may be written as

$$\mathcal{H}_0 = -2J(0)\langle S^z\rangle \sum_i S_i^z - g\mu_B H\sum_i S_i^z - D\sum_i (S_i^z)^2 - J(0)\langle S^z\rangle^2 . \tag{2.3}$$

The interaction Hamiltonian is

$$\mathcal{H}_{\text{int}} = \mathcal{H} - \mathcal{H}_0 = -\sum_{i,j} J_{ij}[(S_i^z - \langle S^z\rangle)(S_j^z - \langle S^z\rangle) + S_i^+ S_j^-] , \tag{2.4}$$

where the thermal average $\langle S^z\rangle$ will be determined self-consistently. The effective-field Hamiltonian has been in the diagonal form. For spin 1, the three molecular-field eigenstates can be designated by their corresponding quantum number of S^z as $|1\rangle$, $|0\rangle$, $|\bar{1}\rangle$. The eigenenergies are, respectively,

$$E_1 = -2J(0)\langle S^z\rangle - g\mu_B H - D , \tag{2.5a}$$

$$E_{\bar{1}} = 2J(0)\langle S^z\rangle + g\mu_B H - D , \tag{2.5b}$$

$$E_0 = 0 .$$

A common constant term $-J(0)\langle S^z\rangle^2$ has been dropped in the energies as only the difference in energies is essential in our calculation. Following I, we define the standard-basis operators $L_{\alpha\eta}$ ($\alpha, \eta = 1, 0, \bar{1}$) taking the effective-field eigenstates as basis. We have

$$\langle\gamma|L_{\alpha\eta}|\xi\rangle = \delta_{\gamma\alpha}\delta_{\eta\xi} , \quad \gamma, \xi = 1, 0, \bar{1} . \tag{2.6}$$

The multiplication rule and the commutation relation for operators on the same site are

$$L_{\alpha\eta}L_{\gamma\xi} = \delta_{\eta\gamma}L_{\alpha\xi} , \tag{2.7a}$$

$$[L_{\alpha\eta}, L_{\gamma\xi}] = \delta_{\eta\gamma}L_{\alpha\xi} - \delta_{\xi\alpha}L_{\gamma\eta} , \tag{2.7b}$$

and operators of different sites commute. Any single-ion operator can be written as a linear combination of the standard-basis operators:

$$O_i = \sum_{\alpha,\gamma}\langle\alpha|O_i|\gamma\rangle L_{\alpha\gamma}^i , \tag{2.8}$$

where the suffix i indicates the site of an ion. The spin operators, for example, can be written as

$$S_i^z = L_{11}^i - L_{\bar{1}\bar{1}}^i , \tag{2.9a}$$

$$(S_i^z)^2 = L_{11}^i + L_{\bar{1}\bar{1}}^i , \tag{2.9b}$$

$$S_i^+ = \sqrt{2}\,(L_{10}^i + L_{0\bar{1}}^i) , \tag{2.9c}$$

$$S_i^- = \sqrt{2}\,(L_{01}^i + L_{\bar{1}0}^i) . \tag{2.9d}$$

The Hamiltonians written in terms of the standard-basis operators are then

$$\mathcal{H}_0 = \sum_{i,\alpha} E_\alpha L_{\alpha\alpha}^i , \tag{2.10}$$

$$\mathcal{H}_{\text{int}} = \sum_{i,j} J_{ij}[(L_{11}^i - L_{\bar{1}\bar{1}}^i - \langle S^z\rangle) \times (L_{11}^j - L_{\bar{1}\bar{1}}^j - \langle S^z\rangle) + 2(L_{10}^i + L_{0\bar{1}}^i)(L_{01}^j + L_{\bar{1}0}^j)] . \tag{2.11}$$

In the interaction representation $L_{\alpha\beta}(\tau) = e^{\mathcal{H}_0\tau}L_{\alpha\beta}e^{-\mathcal{H}_0\tau}$ we obtain the simple τ dependence of the excitation operators,

$$L_{01}(\tau) = e^{-E_1\tau}L_{01} , \tag{2.12a}$$

$$L_{\bar{1}0}(\tau) = e^{E_{\bar{1}}\tau}L_{\bar{1}0} , \tag{2.12b}$$

$$L_{\bar{1}1}(\tau) = e^{E_{\bar{1}}-E_1}L_{\bar{1}1} . \tag{2.12c}$$

We define three noninteracting Green's functions,

$$G_{01}^0(\tau_1 - \tau) \equiv G_1(\tau_1 - \tau) = e^{E_1(\tau_1-\tau)}\begin{cases} n(-E_1) , & \tau > \tau_1 , \\ 1 + n(-E_1) , & \tau < \tau_1 , \end{cases} \tag{2.13a}$$

$$G_{\bar{1}0}^0(\tau_1 - \tau) \equiv G_2(\tau_1 - \tau) = e^{-E_{\bar{1}}(\tau_1-\tau)}\begin{cases} n(E_{\bar{1}}) , & \tau > \tau_1 , \\ 1 + n(E_{\bar{1}}) , & \tau < \tau_1 , \end{cases} \tag{2.13b}$$

$$G_{\bar{1}1}^0(\tau_1 - \tau) \equiv G_3(\tau_1 - \tau) = e^{(E_1-E_{\bar{1}})(\tau_1-\tau)}\begin{cases} n(E_{\bar{1}} - E_1) , & \tau > \tau_1 , \\ 1 + n(E_{\bar{1}} - E_1) , & \tau < \tau_1 , \end{cases} \tag{2.13c}$$

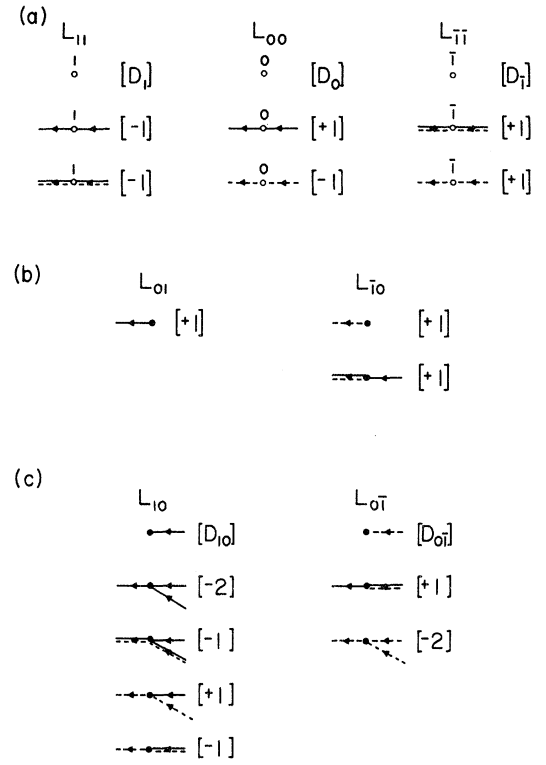

FIG. 1. Vertices corresponding to the standard-basis operators ($S=1$). Vertices corresponding to $L_{1\bar{1}}$ and $L_{\bar{1}1}$, which do not occur in this work, are not shown. The weight factor associated with each vertex is shown in the parentheses.

where $n(x)=(e^{\beta x}-1)^{-1}$. The Wick-like reduction theorem, as shown in I, can now be written as

$$\langle 0_1(\tau_1)\cdots L_{01}(\tau_m=\tau)\cdots 0_n(\tau_n)\rangle_0 = G_1(\tau_1-\tau)\langle [0_1, L_{01}]_{\tau_1}\cdots 0_n(\tau_n)\rangle_0 + \cdots + G_1(\tau_n-\tau)\langle 0_1(\tau_1)\cdots [0_n, L_{01}]_{\tau_n}\rangle_0 . \quad (2.14)$$

A second (third) equation can be obtained with L_{01} replaced by $L_{\bar{1}0}$ ($L_{\bar{1}1}$) and G_1 by G_2 (G_3). In these equations the brackets with the suffix 0 denote the ensemble averages with respect to $\mathcal{H}_0$. Using the reduction theorem, the ensemble average of a T product of n operators can be written as a sum of products of a Green's function and a T product of $n-1$ operators. Repetition of this process (which we shall call matching) gives us finally a summation of products of Green's functions and an ensemble average of products of diagonal operators ($L_{\alpha\alpha}$) over the unperturbed Hamiltonian. Each of such terms can then be represented by a diagram or a set of diagrams with appropriate weight factors (the details have been given in I).

As discussed in I, the lack of uniqueness prevails in the representation of a thermal average of a T product. A priority rule, though arbitrary, can facilitate the drawing of a consistent set of diagrams. In this calculation we shall assign matching priority to the "active operators" in the order L_{01}, $L_{\bar{1}1}$, and $L_{\bar{1}0}$. That is, in applying the reduction theorem, L_{01} is to match with all other operators first, then $L_{\bar{1}1}$ would start to match with other operators, etc. The vertices are summarized in Figs. 1(a)–1(c) with the weight factors shown in the parentheses. The diagonal vertices $L_{\alpha\alpha}$ are represented by small circles and are labeled by α. The Green's functions are not labeled as in I; they are shown in solid line, dashed line, and double line for G_1, G_2, and G_3.

The diagrams are made of vertices, Green's-function lines, interaction lines, and ovals which are used to embrace the vertices of a common site. Vertices are joined together through Green's-function lines and ovals to form a single-site *block*. The diagrams are then formed by linking together the blocks with interaction lines.

The contributions of diagrams are calculated in the Fourier space as usual. We define the Fourier transform of a Green's function:

$$G(\tau)=\sum_n e^{-i\omega_n\tau}G(\omega_n) , \quad (2.15)$$

$$\omega_n=2\pi n/\beta , \quad \beta=1/k_BT ,$$

$$G(\omega_n)=\frac{1}{2\beta}\int_{-\beta}^{\beta}G(\tau)\,e^{i\omega_n\tau}\,d\tau , \quad (2.16)$$

and we obtain the noninteracting Green's functions in the Fourier space

$$G_1(\omega_n)=\frac{1}{\beta}\frac{1}{-i\omega_n-E_1} , \quad (2.17a)$$

$$G_2(\omega_n)=\frac{1}{\beta}\frac{1}{-i\omega_n+E_{\bar{1}}} , \quad (2.17b)$$

$$G_3(\omega_n)=\frac{1}{\beta}\frac{1}{-i\omega_n+E_{\bar{1}}-E_1} . \quad (2.17c)$$

The rules for evaluation of a diagram can now be given.

(i) Assign a frequency to each Green's-function line and a momentum to each interaction line such that the frequencies are conserved at each vertex and the momenta are conserved on each block.

(ii) Associate the solid-line, dashed-line, and double-line Green's functions with $G_\alpha(\omega_n)$ for $\alpha=1$, 2, 3, respectively. Associate with each interaction line a factor $2\beta J(q)$.

(iii) Associate with each block consisting of n_m vertices carrying minus signs, n_t vertices carrying factors 2 or -2, n_α vertices carrying weight factors D_α, and $n_{\alpha\gamma}$ vertices carrying weight factors $D_{\alpha\gamma}$ a weight factor (see I for notations)

$$(-1)^{n_m}2^{n_t}\partial_\alpha^{n_\alpha}\cdots\partial_\gamma^{n_\gamma}\partial_{\alpha\delta}^{n_{\alpha\delta}}\cdots\partial_{\gamma\sigma}^{n_{\gamma\sigma}}(\ln Z_0) .$$

(iv) Multiply all the factors and divide it by the

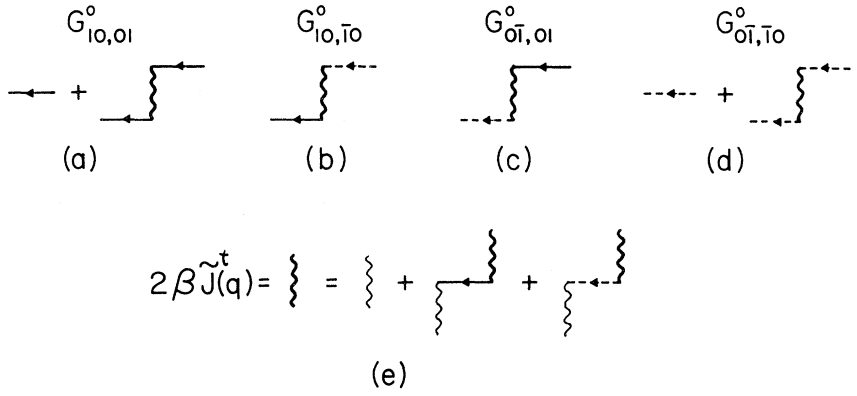

FIG. 2. Diagrams for the zeroth-order Green's functions and the chain-renormalized transverse interaction (in heavy wavy line). The light wavy line depicts a single transverse interaction.

symmetry factor of the diagram. Sum over all internal frequencies and integrate over all internal momenta.

III. ZEROTH-ORDER CALCULATION OF GREEN'S FUNCTIONS AND CORRELATION FUNCTIONS

We first consider the Green's function $G^{10}_{01}(q, \omega_n)$, the $q-\omega_n$ component of $\langle T_\tau \tilde{L}^i_{10}(\tau)\tilde{L}^j_{01}(0)\rangle$. To the zeroth order in $1/z$, the only diagrams aside from the single unperturbed Green's-function line are the chainlike diagrams. These diagrams are shown in Fig. 2(a). The chainlike diagrams can be summed with the help of the renormalized interaction defined in Fig. 2(e). The chain-renormalized transverse interaction, represented by a heavy wavy line, carries a factor $2\beta\tilde{J}^t_q(\omega_n)$ given by

$$2\beta\tilde{J}^t_q(\omega_n) = \frac{2\beta J(q)}{1-2\beta J(q)[D_{10}G_1(\omega_n)+D_{0\bar{1}}G_2(\omega_n)]} \tag{3.1}$$

$$= \frac{2\beta J(q)(i\omega_n+E_1)(i\omega_n-E_{\bar{1}})}{(i\omega_n-\omega^+_q)(i\omega_n-\omega^-_q)}, \tag{3.2}$$

where

$$\begin{aligned} &D_{ij} = D_i - D_j\,,\\ &D_i = \langle L_{ii}\rangle_0\,,\\ &\omega^\pm_q = 2J(0)\langle S^z\rangle - D_{1\bar{1}}J(q) + g\mu_B H_z\\ &\qquad \pm\{[D_{1\bar{1}}J(q)]^2 + D^2 - 2DJ(q)(D_{10}-D_{0\bar{1}})\}^{1/2}\,. \end{aligned} \tag{3.3}$$

Thus, to this order of approximation we have

$$G^{10}_{01}(q,\omega_n) = D_{10}G_1(\omega_n) + D^2_{10}G^2_1(\omega_n)2\beta\tilde{J}^t_q(\omega_n)$$

$$= -\frac{D_{10}}{\beta}\frac{i\omega_n - E_{\bar{1}} + 2J(q)D_{0\bar{1}}}{(i\omega_n-\omega^+_q)(i\omega_n-\omega^-_q)}\,. \tag{3.4}$$

The analytic continuation to the whole complex ω plane by $i\omega_n \to \omega + i\delta$ gives two poles of the Green's function at $\omega^\pm_q$ which are identified as the elementary excitation energies of the system. Notice that $\langle S^z\rangle$ should be calculated to the zeroth order in $1/z$, and that $D_{1\bar{1}} = \langle S^z\rangle_0$, $D_{10} - D_{0\bar{1}} = 3\langle (S^z)^2\rangle_0 - 2$, the spectra can be rewritten as

$$\begin{aligned} \omega^\pm_q &= g\mu_B H_z + \langle S^z\rangle_0[2J(0)-J(q)]\\ &\pm\{D^2 - 2DJ(q)[3\langle (S^z)^2\rangle_0 - 2] + [\langle S^z\rangle_0 J(q)]^2\}^{1/2}\,. \end{aligned} \tag{3.5}$$

The Green's functions $G^{10}_{\bar{1}0}(q,\omega_n)$, $G^{0\bar{1}}_{01}(q,\omega_n)$, and $G^{\bar{1}0}_{0\bar{1}}(q,\omega_n)$ can be calculated in the similar way. The diagrams to the zeroth order in $1/z$ are shown in Figs. 2(b)–2(c). We obtain

$$G^{10}_{\bar{1}0}(q,\omega_n) = G^{0\bar{1}}_{01}(q,\omega_n) = \frac{2J(q)}{\beta}\frac{D_{10}D_{0\bar{1}}}{(i\omega_n-\omega^+_q)(i\omega_n-\omega^-_q)}\,, \tag{3.6}$$

$$G^{0\bar{1}}_{\bar{1}0}(q,\omega_n) = -\frac{D_{0\bar{1}}}{\beta}\frac{i\omega_n+E_1+2J(q)D_{10}}{(i\omega_n-\omega^+_q)(i\omega_n-\omega^-_q)}\,. \tag{3.7}$$

The sum of the four Green's functions gives the $q-\omega_n$ component of the Green's function

$$\langle T_\tau[\tilde{L}^i_{10}(\tau)+\tilde{L}^i_{0\bar{1}}(\tau)][\tilde{L}^j_{01}(0)+\tilde{L}^j_{\bar{1}0}(0)]\rangle\,,$$

which is simply

$$\tfrac{1}{2}\langle T_\tau \tilde{S}^+_i(\tau)\tilde{S}^-_j(0)\rangle_{q,\omega_n}\,.$$

Thus, we have

$$\langle T_\tau \tilde{S}^+_i(\tau)\tilde{S}^-_j(0)\rangle_{q,\omega_n}$$

$$= -\frac{2}{\beta}\frac{D_{1\bar{1}}[i\omega_n - 2J(0)\langle S^z\rangle - g\mu_B H_z] + D(D_{10}-D_{0\bar{1}})}{(i\omega_n-\omega^+_q)(i\omega_n-\omega^-_q)}\,. \tag{3.8}$$

Another combination of the four Green's functions gives

$$\langle T_\tau \tilde{S}^+_i(\tau)[\tilde{S}^-_j(0)\tilde{S}^z_j(0) + \tilde{S}^z_j(0)\tilde{S}^-_j(0)]\rangle_{q,\omega_n}$$

$$= 2\langle T_\tau[\tilde{L}^i_{10}(\tau) - \tilde{L}^i_{0\bar{1}}(\tau)][\tilde{L}^j_{01}(0)+\tilde{L}^j_{\bar{1}0}(0)]\rangle_{q,\omega_n}$$

$$= -\frac{2}{\beta}\frac{(D_{10}-D_{0\bar{1}})[i\omega - 2J(0)\langle S^z\rangle - g\mu_B H_z] + DD_{1\bar{1}}}{(i\omega_n-\omega^+_q)(i\omega_n-\omega^-_q)}\,. \tag{3.9}$$

These Green's functions are related to the corresponding double-time temperature-dependent retarded Green's functions used in Refs. 3–6. If we replace $D_{1\bar{1}}$ by $\langle S^z\rangle$ and $D_{10}-D_{0\bar{1}}$ by $3\langle (S^z)^2\rangle - 2$, we reproduce exactly the results of Refs. 3–6. It is important, however, to note that from these Green's

functions $\langle S^z\rangle$ and $\langle (S^z)^2\rangle$ can only be calculated to the zeroth order in $1/z$. If one determines these quantities "self-consistently" from the Green's functions, as is generally done in the equation-of-motion technique, inconsistency may arise. We shall dwell more upon this subject in the following.

In the Green's-function theory using the equation-of-motion technique, the equal-time autocorrelation functions are calculated from the corresponding approximate Green's functions. For example, from the Green's functions given in Eqs. (3.8) and (3.9), or the corresponding double-time temperature-dependent Green's functions, $\langle S^+S^-\rangle$ and $\langle S^+(S^-S^z+S^zS^-)\rangle$ are calculated. Then with the identities

$$\langle S^+S^-\rangle = \langle S^z\rangle - \langle (S^z)^2\rangle + 2 , \tag{3.10}$$

$$\langle S^+(S^-S^z+S^zS^-)\rangle = \langle S^z\rangle + 3\langle (S^z)^2\rangle - 2 , \tag{3.11}$$

the two quantities $\langle S^z\rangle$ and $\langle (S^z)^2\rangle$ are determined. There does not seem to be any inconsistency until one considers the Green's function

$$\langle T_\tau\{[\tilde{S}_i^+(\tau)\tilde{S}_i^z(\tau)+\tilde{S}_i^z(\tau)\tilde{S}_i^+(\tau)][\tilde{S}_j^-(0)\tilde{S}_j^z(0)+\tilde{S}_j^z(0)\tilde{S}_j^-(0)]]\rangle = 2\langle T_\tau\{[\tilde{L}_{1\bar{0}}^i(\tau)-\tilde{L}_{0\bar{1}}^i(\tau)][\tilde{L}_{01}^j(0)-\tilde{L}_{\bar{1}0}^j(0)]]\rangle , \tag{3.12}$$

and calculates the corresponding autocorrelation function at $\tau=0^+$, $\langle (S^+S^z+S^zS^+)(S^-S^z+S^zS^-)\rangle$. With the help of the commutation relations of spin operators, one can show that $(S^+S^z+S^zS^+)(S^-S^z+S^zS^-)=S^+S^-$. On the other hand,

$$\langle T_\tau\{[\tilde{S}_i^+(\tau)\tilde{S}_i^z(\tau)+\tilde{S}_i^z(\tau)\tilde{S}_i^+(\tau)][\tilde{S}_j^-(0)\tilde{S}_j^z(0)+\tilde{S}_j^z(0)\tilde{S}_j^-(0)]]\rangle - \langle T_\tau[\tilde{S}_j^+(\tau)\tilde{S}_j^-(0)]]\rangle = 4(G_{01}^{0\bar{1}}+G_{\bar{1}0}^{10}) . \tag{3.13}$$

If one uses the results obtained in Eq. (3.6) with the replacements $D_{1\bar{1}}\to\langle S^z\rangle$, $D_{10}-D_{0\bar{1}}\to 3\langle (S^z)^2\rangle - 2$ (i.e., the RPA results in the equation-of-motion calculations), one obtains

$$\langle (S^+S^z+S^zS^+)(S^-S^z+S^zS^-)\rangle - \langle S^+S^-\rangle = -4\{\langle S^z\rangle^2 - [3\langle (S^z)^2\rangle - 2]^2\}\sum_q \frac{J(q)}{\omega_q^+-\omega_q^-}\left(\frac{1}{e^{\beta\omega_q^+}-1}-\frac{1}{e^{\beta\omega_q^-}-1}\right), \tag{3.14}$$

which is evidently not zero. This points to the fact that a correlation function may take different values when it is calculated from different Green's functions; the values of $\langle S^z\rangle$ and $\langle (S^z)^2\rangle$ depend on the set of Green's functions used in the calculation and are not uniquely determined. This redundancy in the Green's-function calculation was first pointed out explicitly by Murao and Matsubara.[2] Unfortunately, in the equation-of-motion technique $\langle S^z\rangle$ and $\langle (S^z)^2\rangle$ can only be calculated from the Green's functions in the way described above. While Murao and Matsubara[2] chose Eqs. (3.11) and (3.12) to determine $\langle S^z\rangle$ and $\langle (S^z)^2\rangle$, the others[3-6] used Eqs. (3.10) and (3.11). To remove or to reduce the inconsistency requires an improvement of the decoupling scheme, which is usually rather difficult. On the other hand, in the diagrammatic approach, such inconsistency will not occur provided that one sums all the diagrams to a given order. The discrepancy we have shown is, in the terms of diagrammatic expansion, simply owing to the inconsistent inclusion of only some of the higher-order terms. To be more explicit, we note that in the calculation of the autocorrelation functions from the Green's functions a summation over the external momentum is performed. The first diagram in the Green's function (the noninteracting Green's function) is independent of momentum and gives a term of the zeroth order in $1/z$ for the autocorrelation function; but, the other chainlike diagrams contribute terms of the first order in $1/z$ to the autocorrelation function because of the summation over the momentum variable. Not all first-order terms in $1/z$ have been collected however. All diagrams classified as first order in $1/z$ in the expansion of the Green's function have been dropped. Some of these diagrams would contribute to the autocorrelation function to the first order in $1/z$ and have to be included along with the chainlike diagrams in the calculation. Ignoring the contribution of the chainlike diagrams (in the zeroth-order calculation) both $\langle S^+S^-\rangle$ and $\langle (S^+S^z+S^zS^+)(S^-S^z+S^zS^-)\rangle$ are equal to $\langle S^z\rangle_0 - \langle (S^z)^2\rangle_0 + 2$, as expected. In the higher-order calculations all diagrams contributing to that order should be included and the two autocorrelation functions will then be equal to each other. We recall that the difference of the two Green's functions giving rise to a difference for the two correlation functions is $4(G_{01}^{0\bar{1}}+G_{\bar{1}0}^{10})$. To the zeroth order the equal-time autocorrelation function $\langle L_{0\bar{1}}L_{01}\rangle$ and $\langle L_{1\bar{0}}L_{\bar{1}0}\rangle$ are identically zero because of the lack of noninteracting Green's functions for $G_{01}^{0\bar{1}}$ and $G_{\bar{1}0}^{10}$. It will be shown in Sec. IV that after collecting all the diagrams which contribute to the first order in $1/z$ (one momentum summation), the two correlation functions are identically zero again. *The consistency in each order lends a strong support to the classification of the diagrams according to the number of momentum variables summed over in the diagram.*

IV. FIRST-ORDER CALCULATION OF GREEN'S FUNCTIONS AND CORRELATION FUNCTIONS

As discussed in I, the summation of diagrams can be done using a modified Dyson's equation. If we define an irreducible part as a diagram or part of the diagram which would not break apart by removing one of the interaction lines, a diagram can then be viewed as a set of irreducible parts joined together by single interaction lines. Diagrams can then be summed in terms of the irreducible parts formally, with the modified Dyson's equation

$$G = \Sigma + \Sigma V G \,, \tag{4.1}$$

where Σ represents the collection of the irreducible parts, and V the interaction potential.

We now turn to the Green's function

$$G_{01}^{10}(q, \omega_n) \equiv \langle T_\tau \tilde{L}_{10}^{i}(\tau) \tilde{L}_{01}^{j}(0) \rangle_{q, \omega_n} \,. \tag{4.2}$$

Since G_{01}^{10} couples with $G_{01}^{0\bar{1}}$, $G_{\bar{1}0}^{10}$, and $G_{\bar{1}0}^{0\bar{1}}$, we consider the matrix Green's function G with the four Green's functions as the matrix elements. Summation of the diagrams in terms of the irreducible parts gives

$$G = \Sigma + \Sigma[2\beta J(q)]G \,, \tag{4.3}$$

where Σ is now a matrix consisting of elements Σ_{01}^{10}, $\Sigma_{01}^{0\bar{1}}$, $\Sigma_{\bar{1}0}^{10}$, and $\Sigma_{\bar{1}0}^{0\bar{1}}$, where Σ_{ab}^{cd} is the collection of irreducible parts with starting vertex L_{ab} and terminating vertex L_{cd}. Solving the matrix equation, we obtain

$$\begin{pmatrix} G_{01}^{10} & G_{01}^{0\bar{1}} \\ G_{\bar{1}0}^{10} & G_{\bar{1}0}^{0\bar{1}} \end{pmatrix} = \frac{1}{Q} \begin{pmatrix} 1 - 2\beta J(q)(\Sigma_{\bar{1}0}^{10} + \Sigma_{\bar{1}0}^{0\bar{1}}) & 2\beta J(q)(\Sigma_{01}^{10} + \Sigma_{01}^{0\bar{1}}) \\ 2\beta J(q)(\Sigma_{\bar{1}0}^{10} + \Sigma_{\bar{1}0}^{0\bar{1}}) & 1 - 2\beta J(q)(\Sigma_{01}^{10} + \Sigma_{01}^{0\bar{1}}) \end{pmatrix} \begin{pmatrix} \Sigma_{01}^{10} & \Sigma_{01}^{0\bar{1}} \\ \Sigma_{\bar{1}0}^{10} & \Sigma_{\bar{1}0}^{0\bar{1}} \end{pmatrix}, \tag{4.4}$$

where

$$Q = 1 - 2\beta J(q)(\Sigma_{01}^{10} + \Sigma_{01}^{0\bar{1}} + \Sigma_{\bar{1}0}^{10} + \Sigma_{\bar{1}0}^{0\bar{1}}) \,. \tag{4.5}$$

The arguments q and ω_n of the Green's functions and the irreducible parts have been deleted in the equations for simplicity. The transverse-spin Green's function $\langle T_\tau \tilde{S}_i^+(\tau) \tilde{S}_j^-(0) \rangle_{q, \omega_n}$ can now be written as the sum of the four Green's functions and we have

$$\langle T_\tau \tilde{S}_i^+(\tau) \tilde{S}_j^-(0) \rangle_{q, \omega_n} = \frac{\Sigma_{01}^{10} + \Sigma_{01}^{0\bar{1}} + \Sigma_{\bar{1}0}^{10} + \Sigma_{\bar{1}0}^{0\bar{1}}}{1 - 2\beta J(q)(\Sigma_{01}^{10} + \Sigma_{01}^{0\bar{1}} + \Sigma_{\bar{1}0}^{10} + \Sigma_{\bar{1}0}^{0\bar{1}})} \,. \tag{4.6}$$

The poles of the Green's function analytically continued to the whole ω plane give the spin-wave energies, which can be found by solving

$$Q = 1 - 2\beta J(q)(\Sigma_{01}^{10} + \Sigma_{01}^{0\bar{1}} + \Sigma_{\bar{1}0}^{10} + \Sigma_{\bar{1}0}^{0\bar{1}}) = 0 \,. \tag{4.7}$$

To the zeroth order in $1/z$, $\Sigma_{01}^{10} = D_{10} G_1$, $\Sigma_{\bar{1}0}^{0\bar{1}} = D_{0\bar{1}} G_2$, and $\Sigma_{01}^{0\bar{1}} = \Sigma_{\bar{1}0}^{10} = 0$; the results given in Eq. (3.5) of Sec. III are recovered.

To the first order in $1/z$, we collect all the single-loop irreducible parts as Σ. The spin-wave energy and the Green's function will then be correct to the first order in $1/z$. Using the vertices shown in Fig. 1, diagrams for the irreducible parts Σ_{01}^{10} to the first order in $1/z$ are constructed. These diagrams are shown in Fig. 3. Diagrams which contain blocks connected by a zero-momentum-transfer interaction line are deleted. They sum to zero. This is because the self-consistent-field term $2J(0)\langle S^z \rangle \sum_i S_i^z$ has been separated from the exchange-interaction Hamiltonian and included in the unperturbed Hamiltonian. (The longitudinal-interaction vertices then becomes $S^z - \langle S^z \rangle$ with $\langle S^z \rangle$ determined self-consistently.) The heavy wavy lines represent the renormalized transverse interactions which have been discussed in Sec. III. The renormalization of the longitudinal exchange interaction is similarly achieved. This is shown diagrammatically in Fig. 4, where the renormalized longitudinal interaction is represented by a heavy wavy line connecting the diagonal vertices $L_{11}^{i} - L_{\bar{1}\bar{1}}^{i} - \langle S^z \rangle$ denoted by small circles. We obtain

$$2\beta \tilde{J}_l(q, \omega_n) = \frac{2\beta J(q)}{1 - 2\beta J(q)(D_1 + D_{\bar{1}} - D_{1\bar{1}}^2)} \,. \tag{4.8}$$

Diagrams for $\Sigma_{\bar{1}0}^{0\bar{1}}$ can be found similarly. They are, in fact, the same diagrams as those shown in Fig. 3 with all solid lines in the diagrams replaced by dashed lines and *vice versa* except for diagrams (*l*), (*m*), (*n*). The three corresponding diagrams of $\Sigma_{\bar{1}0}^{0\bar{1}}$ which conform to the priority rule are shown in Fig. 5(a). They are quite different from the three diagrams obtained from Fig. 3 (*l*), (*m*), (*n*) by interchanging the solid lines and the dashed lines as shown in Fig. 5(b). The latter three diagrams are, however, obtainable by reversing the priority rule. Since the priority rule is arbitrary and the sum of these two sets of diagrams are equal, we are free to replace the diagrams in set 5(a) by those in set 5(b). Diagrams of $\Sigma_{01}^{0\bar{1}}$ are shown in Fig. 6. Again, interchanging the solid lines and dashed lines in each of the diagrams of Fig. 6 we obtain all diagrams of $\Sigma_{\bar{1}0}^{10}$.

To find the first-order correction to the spin-wave energies we first write Σ's in the following form defining Λ_{ij} and Δ_{ij}:

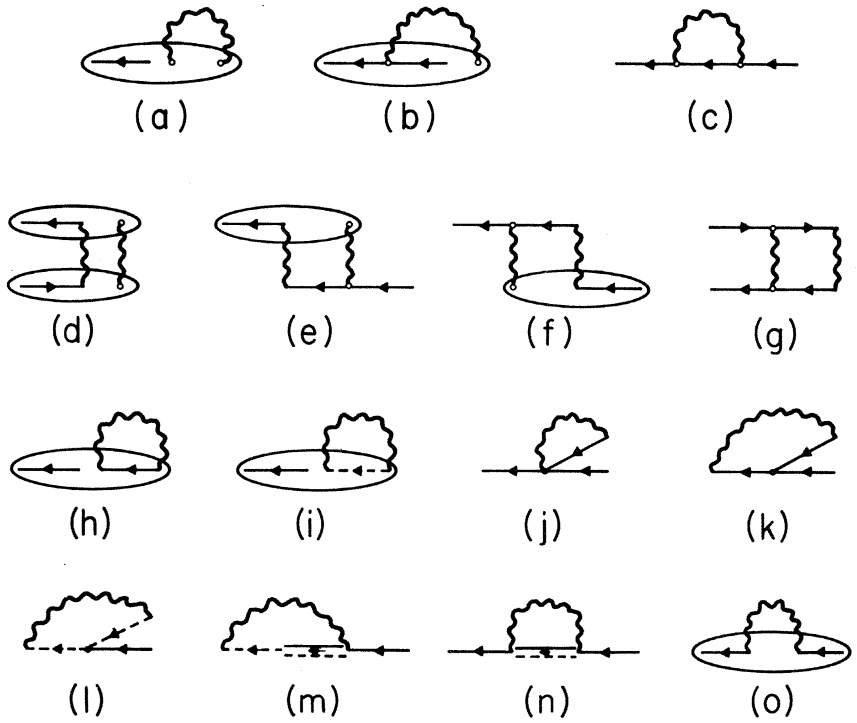

FIG. 3. First-order-correction diagrams for the Green's function $G^{10}_{0\bar{1}}(\omega_n, q)$.

$$\begin{pmatrix} \Sigma^{10}_{01} & \Sigma^{0\bar{1}}_{01} \\ \Sigma^{10}_{\bar{1}0} & \Sigma^{0\bar{1}}_{\bar{1}0} \end{pmatrix} = \begin{pmatrix} (D_{10}+\Lambda_{11})G_1 + \Delta_{11}G_1^2 & \Lambda_{12}G_1 + \Delta_{12}G_1G_2 \\ \Lambda_{21}G_2 + \Delta_{21}G_1G_2 & (D_{0\bar{1}}+\Lambda_{22})G_2 + \Delta_{22}G_2^2 \end{pmatrix}, \tag{4.9}$$

where the Λ's and Δ's are functions of ω_n and q. Solution of Eq. (4.6) to the first order in $1/z$ can be found as

$$\tilde{\omega}_q^{\pm} = 2J(0)\langle S^z\rangle - (A_q + B_q) \pm [(A_q + B_q)^2 + D^2 - 2D(A_q - B_q) + C_q]^{1/2}, \tag{4.10}$$

where

$$A_q = J(q)(D_{10} + \Lambda_{11} + \Lambda_{12}) + (1/2\beta)(\Delta_{11}/D_{10}), \tag{4.11a}$$

$$B_q = J(q)(D_{0\bar{1}} + \Lambda_{21} + \Lambda_{22}) + (1/2\beta)(\Delta_{22}/D_{0\bar{1}}), \tag{4.11b}$$

$$C_q = \frac{2J(q)}{\beta}\left(\Delta_{12} + \Delta_{21} - \frac{D_{0\bar{1}}}{D_{10}}\Delta_{11} - \frac{D_{10}}{D_{0\bar{1}}}\Delta_{22}\right), \tag{4.11c}$$

and the Λ's and Δ's are evaluated at $\omega = \omega_q^{\pm}$, the zeroth-order frequencies.

Since the explicit results for general temperature are rather lengthy, we only present the results in the low-temperature limit. For $2J(0)\beta \gg 1$, we can set $D_1 = 1$, $D_0 = D_{\bar{1}} = 0$. Equation (4.10) then reduces to

$$\tilde{\omega}_q^{\pm} = \omega_q^{\pm} - J(q)(\Lambda_{11} + \Lambda_{22} + \Lambda_{12}) - \frac{1}{2}\frac{\Delta_{11}}{\beta} \pm \frac{1}{2}\frac{1}{|J(q) - D|} \times \left(2J^2(q)(\Lambda_{11} + \Lambda_{22} + \Lambda_{12}) - 2DJ(q)(\Lambda_{11} - \Lambda_{22} + \Lambda_{12}) + \frac{\Delta_{11}}{\beta}[J(q) - D] + 2J(q)\frac{\Delta_{21}}{\beta}\right). \tag{4.12}$$

After evaluations of the Λ's and the Δ's using the Poisson's sum rule,[17] we find

$$\tilde{\omega}_q^{-} = \omega_q^{-} - \frac{2}{N}\sum_k n(\omega_k^{-})\left(\frac{D[J(q) + J(k)]}{J(q) + J(k) - D} + J(0) + J(k-q) - J(q) - J(k)\right), \tag{4.13}$$

$$\tilde{\omega}_q^{+} = \omega_q^{+}, \tag{4.14}$$

which agree completely with those given by Kashchenko *et al.*[14] The spin-wave damping has been calculated by these authors also. To the zeroth order in $1/z$, there is no damping; to the first or-

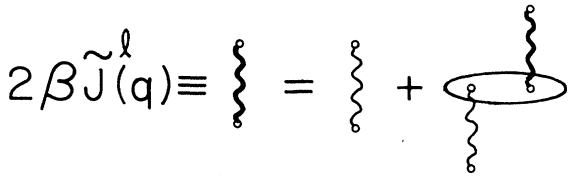

FIG. 4. Diagram for the chain-renormalized longitudinal interaction (in heavy wavy line). The light wavy line depicts a single longitudinal interaction.

der in $1/z$ the damping of spin waves is due to the scattering by the S^z fluctuations which is small at low temperatures but significant near T_c. The results have been given near T_c for both the weak-field and the strong-field cases. We shall not elaborate on this.

Correlation functions can be obtained from the corresponding Green's functions. However, in the calculation of autocorrelation functions some caution is necessary to avoid any incomplete inclusion of terms of higher order. Self-consistency and preservation of kinematic conditions can be maintained in each and every order of approximation only if diagrams are summed consistently. We illustrate this with the calculation of the autocorrelation function $\langle \tilde{L}^i_{0\bar{1}}(\tau)\tilde{L}^i_{01}(0)\rangle$ as $\tau \to 0^+$. From physical considerations, the function should be identically zero since it calls for excitation to the level $|0\rangle$ of the same ion twice at the same time. The RPA calculation, however, shows a finite value and therefore creates the inconsistency that the values of $\langle S^z\rangle$ and $\langle (S^z)^2\rangle$ would depend on the set of Green's functions chosen in the calculation. To calculate this autocorrelation function in the diagrammatic method, we consider the diagrams of the corresponding Green's function $\langle T_\tau \tilde{L}^i_{0\bar{1}}(\tau)\tilde{L}^i_{01}(0)\rangle_{q,\omega_n}$ and sum over ω_n and q. In this procedure, first of all, the zeroth-order chainlike diagrams of the Green's function give a term of first order in $1/z$ to the correlation function because of the momentum sum. This is, however, not the only term of order $1/z$ in the correlation function. There are four first-order diagrams in the Green's function, which contribute to the autocorrelation function to the same order. The four diagrams are those in Figs. 6(e)–6(h). Their contributions are, respectively,

$$\frac{1}{N}D_{0\bar{1}}\sum_{\omega_n,\omega_m,q} 2\beta\tilde{J}^t_q(\omega_n)G_2(\omega_n)G_1(\omega_m)G_2(\omega_m)\ ,$$

$$\frac{1}{N}D_{10}\sum_{\omega_n,\omega_m,q} 2\beta\tilde{J}^t_q(\omega_n)G_1(\omega_n)G_3(\omega_n+\omega_m)G_1(\omega_m)\ ,$$

$$-\frac{1}{N}D_{0\bar{1}}\sum_{\omega_n,\omega_m,q} 2\beta\tilde{J}^t_q(\omega_n)G_3(\omega_n+\omega_m)G_1(\omega_m)G_2(\omega_m)\ ,$$

$$-\frac{1}{N}(D_0+D_{10}D_{0\bar{1}})\sum_{\omega_n,q} 2\beta\tilde{J}^t_q(\omega_n)G_1(\omega_n)G_2(\omega_n)\ .$$

Using the Poisson's sum rule[17] we carry out the frequency sums. The sum of these four diagrams cancels out the contribution of the chainlike diagrams exactly. We obtain therefore, according to present classification of the diagrams, the kinematical condition $\langle L^i_{10}L^i_{\bar{1}0}\rangle = 0$ to the zeroth and first orders. No inconsistency can arise and all physical quantities are uniquely determined. While the preservation of kinematics is expected in each order and to all orders of calculation, a general proof is however lacking at present.

V. THERMODYNAMICS OF THE UNIAXIAL FERROMAGNET WITH SINGLE-ION ANISOTROPY

Any single-ion physical quantity can be calculated in terms of the thermal averages of the three diagonal operators $\langle L_{\alpha\alpha}\rangle$ ($\alpha = 1, 0, \bar{1}$), which describe the populations of the three molecular-field states used as the basis states. We denote $\langle L_{\alpha\alpha}\rangle$ by P_α ($\alpha = 1, 0, \bar{1}$). To the zeroth order in $1/z$, they are D_α, the molecular-field-theory (MFT) results. The first-order correction to P_1 is given by the four diagrams shown in Fig. 7 where the circle in each diagram represents an L_{11} vertex. The heavy wavy lines are known to represent the chain-renormalized interactions. The circles which attach to the ends of the logitudinal-interaction lines depict the diagonal vertices $L_{11} - L_{\bar{1}\bar{1}} - \langle S^z\rangle$ as before. We obtain after summing over the frequency in each diagram

$$P_1 = D_1 + \tfrac{1}{2}D_1(1 - D_1 - D_{\bar{1}} - 2D_{1\bar{1}} + 2D^2_{1\bar{1}})\frac{1}{N}\sum_q \frac{2\beta J(q)}{1 - 2\beta J(q)(D_1 + D_{\bar{1}} - D^2_{1\bar{1}})}$$
$$+ \frac{1}{N}\sum_q [1 - 2\beta J(q)D_1(1 - D_{10})]f(q) + \frac{1}{N}\sum_q 2\beta J(q)D_1D_{0\bar{1}}g(q) - D_1D_{0\bar{1}}(1 - 2D_{10})\frac{1}{N}\sum_q h(q)\ , \tag{5.1}$$

where

$$f(q) = 2J(q)\left[\frac{D_{10}}{\omega^+_q - \omega^-_q}\left(n(\omega^+_q)\frac{\omega^+_q - E_{\bar{1}}}{\omega^+_q + E_1} - n(\omega^-_q)\frac{\omega^-_q - E_{\bar{1}}}{\omega^-_q + E_1}\right) + \frac{2DD_0}{(\omega^+_q + E_1)(\omega^-_q + E_1)}\right], \tag{5.2a}$$

$$g(q) = 2J(q)\left[\frac{D_{0\bar{1}}}{\omega^+_q - \omega^-_q}\left(n(\omega^+_q)\frac{\omega^+_q + E_1}{\omega^+_q - E_{\bar{1}}} - n(\omega^-_q)\frac{\omega^-_q + E_1}{\omega^-_q - E_{\bar{1}}}\right) - \frac{2DD_{\bar{1}}}{(\omega^+_q - E_{\bar{1}})(\omega^-_q - E_{\bar{1}})}\right], \tag{5.2b}$$

$$h(q)=\frac{\beta[2J(q)]^2}{\omega_q^+-\omega_q^-}[n(\omega_q^+)-n(\omega_q^-)]\ . \tag{5.2c}$$

Similarly we calculate $P_{\bar{1}}$ to the first order in $1/z$, the diagrams are the same as those given in Fig. 7 except that the solid lines in diagram 7(d) are replaced by dashed lines and that the circle in each diagram (which are not attached to the wavy line) now represents the vertex $L_{\bar{1}\bar{1}}$. We find

$$P_{\bar{1}}=D_{\bar{1}}+\tfrac{1}{2}D_{\bar{1}}(1-D_1-D_{\bar{1}}+2D_{1\bar{1}}+2D_{1\bar{1}}^2)\frac{1}{N}\sum_q\frac{2\beta J(q)}{1-2\beta J(q)(D_1+D_{\bar{1}}-D_{1\bar{1}}^2)}+\frac{1}{N}\sum_q 2\beta J(q)D_{\bar{1}}D_{10}f(q)$$
$$-\frac{1}{N}\sum[1-2J(q)D_{\bar{1}}(1+D_{0\bar{1}})]g(q)+D_{\bar{1}}D_{10}(1-2D_{0\bar{1}})\frac{1}{N}\sum_q h(q)\ . \tag{5.3}$$

P_0 can also be calculated with the same diagrams given in Fig. 7 plus the diagram 7(d) used in the calculation of $P_{\bar{1}}$ (diagram 7(d) with solid lines replaced by dashed lines). Clearly, the circles (not attached to the wavy lines) on each diagram now represent the vertices L_{00}. The result is simply

$$P_0=1-P_1-P_{\bar{1}}\ , \tag{5.4}$$

and the sum rule $\sum_\alpha L_{\alpha\alpha}=1$ is satisfied.

A. Curie temperature of an anisotropic ferromagnet

The magnetization $\langle S^z\rangle$ and the quadrupole moment $\langle(S^z)^2\rangle$ are given by $P_1-P_{\bar{1}}$ and $P_1+P_{\bar{1}}=1-P_0$, respectively. Setting the external magnetic field equal to zero and considering the small $\langle S^z\rangle$ limit in the equation

$$\langle S^z\rangle=P_1-P_{\bar{1}}\ , \tag{5.5}$$

we find the Curie temperature:

$$\frac{1}{2\beta_cJ(0)}=\frac{2}{\gamma}+\frac{2}{\gamma}(1-6/\gamma)\frac{1}{N}\sum_q\frac{\beta_cJ(q)}{1-(4/\gamma)\beta_cJ(q)}$$
$$+\frac{2}{N}\sum_q\frac{e^{-\beta_cb}}{(1-e^{-\beta_cb})^2}\left(1-\frac{2\beta_cJ(q)}{\gamma}\right)^2$$
$$+\frac{1}{N}\sum_q\frac{2}{\gamma^2}\frac{\beta_cJ(q)}{b}[3D(\gamma-2)-2J(q)]\frac{1+e^{-\beta_cb}}{1-e^{-\beta_cb}}$$
$$-2\frac{e^{-\beta_cD}}{(e^{-\beta_cD}-1)^2}\ , \tag{5.6}$$

where

$$\beta_c=\frac{1}{kT_c}\ , \tag{5.7a}$$

$$\gamma=2+e^{-\beta_cD}\ , \tag{5.7b}$$

and

$$b^2=D^2+4DJ(q)(1-3/\gamma)\ . \tag{5.7c}$$

The result in the MFT is obtained by keeping only the first term on the right-hand side of the equation; the other terms represent the first-order correction.

For weak anistropy $[D\ll J(0)]$, to the first order in D, Eq. (5.6) reduces to

$$\frac{1}{2\beta_cJ(0)}=\frac{2}{3}-\frac{10}{9N}\sum_q\frac{\beta_cJ(q)}{1-\frac{4}{3}\beta_cJ(q)}-\frac{4}{27}\frac{1}{N}\sum_q(\beta_cJ_q)^2$$
$$+\beta_cD\left(\frac{2}{9}-\frac{8}{81}\frac{1}{N}\sum_q[\beta_cJ(q)]^2\right.$$
$$\left.-\frac{1}{N}\sum_q\frac{\frac{7}{9}\beta_cJ(q)}{1-\frac{4}{3}\beta_cJ(q)}-\frac{1}{N}\sum_q\frac{\frac{16}{81}[\beta_cJ(q)]^2}{[1-\frac{4}{3}\beta_cJ(q)]^2}\right)\ . \tag{5.8}$$

Putting $D=0$, and substituting for β_c in the correction terms by its zero-order value (MFT), this equation gives the result obtained by Vaks, Larkin, and Pikin (VLP)[10] for the isotropic Heisenberg ferromagnet. Equation (5.8) then represents the effect of the anisotropy to the first order of β_cD.

In the other extreme limit, for $D\gg J(0)$, we expand the terms in Eq. (5.6) in powers of D^{-1} and we obtain

$$\frac{1}{2\beta_cJ(0)}=1-\frac{1}{N}\sum_q\frac{2\beta_cJ(q)}{1-2\beta_cJ(q)}-\frac{1}{N}\sum\frac{\beta_cJ^2(q)}{D}$$
$$-\frac{1}{N}\sum\frac{\beta_cJ^3(q)}{D^2}+O(D^{-3},e^{-\beta_cD})\ . \tag{5.9}$$

With $J(0)/D\to 0$, the $S^z=0$ state is suppressed and we recover the result obtained by VLP[10] for an Ising system of spin $\frac{1}{2}$ (with an exchange parameter $4J_{ij}$).

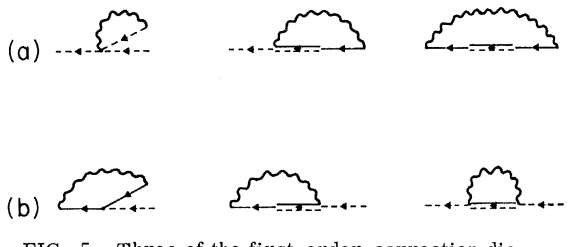

FIG. 5. Three of the first-order-correction diagrams for the Green's function $G_{\bar{1}0}^{0\bar{1}}(\omega_n,q)$. Set (b) gives the diagrams obtained by interchanging the solid lines and the dashed lines in the diagrams of Fig. 3 (l, m, n). These diagrams do not conform to the priority rule. Set (a) shows the corresponding diagrams constructed according to the priority rule.

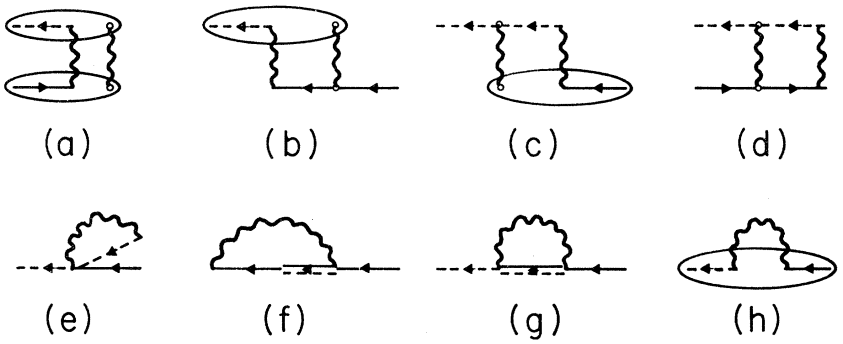

FIG. 6. First-order-correction diagrams for the Green's function $G_{01}^{0\bar{1}}(\omega_n, q)$. Replacing each solid line with a dashed line and *vice versa*, we obtain diagrams for $G_{\bar{1}0}^{10}(\omega_n, q)$.

The spin-1 Ising system with a single-ion anisotropy has been studied recently by the high-temperature-expansion (HTE) technique. To compare with the HTE results we can make a straightforward modification to our calculation allowing an anisotropic exchange interaction. If we multiply the transverse exchange interaction by η and follow the same diagrammatic calculation as above we obtain the equation determining the Curie temperature as

$$\frac{1}{2\beta_c J(0)} = \frac{2}{\gamma} + \frac{2}{\gamma}(1-6/\gamma)\frac{1}{N}\sum_q \frac{\beta_c J(q)}{1-(4/\gamma)\beta_c J(q)} - \frac{2e^{-\beta_c D}}{(e^{-\beta_c D}-1)^2}$$
$$+ \frac{2}{N}\sum_q \left(1-\frac{2\eta\beta_c J(q)}{\gamma}\right)^2 \frac{e^{-\beta_c d}}{(1-e^{-\beta_c d})^2} + \frac{1}{N}\sum_q \frac{2}{\gamma^2}\frac{\eta\beta_c J(q)}{d}[3D(\gamma-2)-2\eta J(q)]\frac{1+e^{-\beta_c d}}{1-e^{-\beta_c d}} . \quad (5.10)$$

Here,

$$d^2 = D^2 + 4D\eta J(q)(1-3/\gamma) . \quad (5.11)$$

This is the most general result for a uniaxial ferromagnet of spin 1. It is valid for $\eta < 1 + D/J(0)$ (in MFT) because a magnetic ordering along the z axis has been assumed.

Setting $\eta = 0$ we obtain an Ising-1 system with a single-ion anisotropy and the equation for the Curie temperature is now

$$\frac{1}{2\beta_c J(0)} = \frac{2}{\gamma} + \frac{2}{\gamma}(1-6/\gamma)\frac{1}{N}\sum_q \frac{\beta_c J(q)}{1-(4/\gamma)\beta_c J(q)} . \quad (5.12)$$

Taking $D = 0$ ($\gamma = 3$) we obtain

$$\frac{1}{2\beta_c J(0)} = \frac{2}{3} - \frac{2}{3}\frac{1}{N}\sum_q \frac{\beta_c J(q)}{1-\frac{4}{3}\beta_c J(q)} , \quad (5.13)$$

which determines T_c for a spin-1 Ising ferromagnet. In the other limit $D/J(0) \to \infty$ we recover again Eq. (5.9) as the system now becomes an Ising ferromagnet of spin $\frac{1}{2}$.

To compare the critical temperatures obtained in the present calculation with the HTE and MFT values, we summarize the values of $k_B T_c/J(0)$ of the three calculations in Table I. [It should be noted that for Ising $\frac{1}{2}$, the exchange parameter is taken as $4J(0)$ instead of $J(0)$. This introduces a factor of 4 to the Ising $\frac{1}{2}$ values in the table.] The percentage values in the parentheses are the percentage deviation of the values from the HTE values. The agreement with the HTE is within a few percent in all cases.

For a general value of single-ion anisotropy, we have plotted the values of $k_B T_c/J(0)$ obtained from Eqs. (5.6) and (5.12), for the Heisenberg and the Ising-1 cases, respectively, in Figs. 8 and 9. The HTE values are shown for the fcc lattice.[21] The values from the MFT are also plotted for comparison.

B. Low-temperature behavior

At low temperatures, when $\beta J(0) \gg 1$, many diagrams can be dropped from the calculation. Indeed only diagrams (d) in Fig. 7 would contribute in the first-order calculation of P_1 if terms of order of $e^{-2\beta J(0)}$ are discarded. We find, to this order

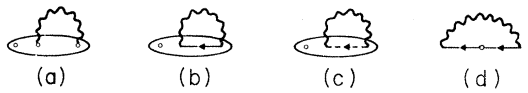

FIG. 7. First-order-correction diagrams in the calculation of the population of molecular-field state $|1\rangle$. Small circles that are not connected to the interaction lines are the L_{11} vertices; those which attach to interaction lines are the $L_{11} - L_{\bar{1}\bar{1}} - \langle S^z \rangle$ vertices.

TABLE I. Values of the critical temperatures from various calculations.

		sc	bcc	fcc
Isotropic Heisenberg	Pres. cal.	0.96 (5%)	1.004 (5%)	1.050 (4%)
	HTE (Ref. 18)	0.9116	0.9571	1.0026
	MFT	1.333	1.333	1.333
Ising $\frac{1}{2}$	Pres. cal.	1.519 (1%)	1.585 (0.2%)	1.628 (0.3%)
	HTE (Ref. 19)	1.5036	1.5884	1.6326
	MFT	2.	2.	2.
Ising 1	Pres. cal.	1.055	1.097	1.122 (1%)
	HTE (Ref. 20)	$\simeq 1.07$	$\simeq 1.12$	1.135
	MFT	1.333	1.333	1.333

$$P_1 = 1 - \frac{1}{N}\sum_q n(\omega_q^-) , \tag{5.14}$$

$$P_0 = 1 - P_1 , \tag{5.15}$$

$$P_{\bar{1}} = 0 , \tag{5.16}$$

and

$$\omega_q^- = 2J(0)(1-\gamma_q) + D + g\mu_B H . \tag{5.17}$$

If we define the reduced temperature τ as

$$\tau \equiv k_B T/8\pi J(0)\alpha , \tag{5.18}$$

the low-temperature expansion of $\langle S^z\rangle$ for a cubic lattice is

$$\langle S^z\rangle = 1 - Z_{3/2}(D+g\mu_B H)\tau^{3/2} + 3\pi(5C_1+3C_2)Z_{5/2}(D+g\mu_B H)\tau^{5/2} - \cdots , \tag{5.19}$$

where the incomplete Riemann ζ function $Z_\lambda(x)$ is defined as

$$Z_\lambda(x) = \sum_{p=1}^{\infty} \frac{e^{-p\beta x}}{p^\lambda} , \tag{5.20}$$

and the constants α, C_1, and C_2 are the coefficients in the expansion of γ_q for the cubic lattices[22]:

$$\gamma_q = 1 - \alpha[q^2 + C_1 q^4 + C_2(q_x^4 + q_y^4 + q_z^4) + \cdots] . \tag{5.21}$$

This is, in fact, identical to the result of the spin-wave theory since the present theory reduces to the simple spin-wave theory in the extreme low-temperature limit where the spin-wave–spin-wave interaction can be ignored. We may also note that the quadrupole moment $\langle (S^z)^2\rangle$, which is equal to $P_1 + P_{\bar{1}}$, is equal to $\langle S^z\rangle$ in this limit.

When temperature is elevated, the effect of the interactions of spin waves manifests itself in the temperature behavior of the magnetization. As Dyson concluded for an isotropic ferromagnetic system, the lowest-order term in the temperature expansion of magnetization due to spin-wave–spin-wave interactions is proportional to T^4.[23] We have investigated the anisotropic case and obtain the leading-order terms due to the spin-wave–spin-wave interactions by carrying out the calculation of $\langle S^z\rangle$ to the second order in the $1/z$ expansion. The second-order diagrams used to calculate P_1 and $P_{\bar{1}}$ are given in Fig. 10. We have shown only the free-energy diagrams. As in the first-order calculation of P_α, the vertex $L_{\alpha\alpha}$ is added to one of the Green's functions in the free-energy diagrams in all possible ways. After summing over the two frequencies we find the second-order correction of $\langle S^z\rangle = P_1 - P_{\bar{1}}$ as

$$\delta^{(2)}\langle S^z\rangle = -\frac{\beta}{N^2}\sum_{k,q}\left(J(0)+J(k-q)-J(k)-J(q)-\frac{D(J(k)+J(q))}{D-J(k)-J(q)}\right)n(\omega_k^-)n(\omega_q^-)[2+n(\omega_k^-)+n(\omega_q^-)] . \tag{5.22}$$

It should be noted that the first term here arises from the first-order-correction diagram, due to the self-consistent determination of $\langle S^z\rangle$.

For an isotropic ferromagnet $D=0$ and $H=0$, the leading-order term in the temperature is

$$6\pi(5C_1+3C_2)Z_{3/2}(0)Z_{5/2}(0)\tau^4 , \tag{5.23}$$

which agrees with Dyson's result to the first Born approximation.[23] In the presence of a single-ion anisotropy we find

$$\delta^{(2)}\langle S^z\rangle = 6\pi(5C_1+3C_2)Z_{3/2}(D+g\mu_B H)Z_{5/2}(D+g\mu_B H)\tau^4 - \frac{1}{2\pi\alpha}\frac{D}{2J(0)-D}Z_{1/2}(D+g\mu_B H)Z_{3/2}(D+g\mu_B H)\tau^2 - 3\left(\frac{D}{2J(0)-D}\right)^2[Z_{3/2}^2(D+g\mu_B H)+Z_{5/2}(D+g\mu_B H)Z_{1/2}(D+g\mu_B H)]\tau^3 + \cdots . \tag{5.24}$$

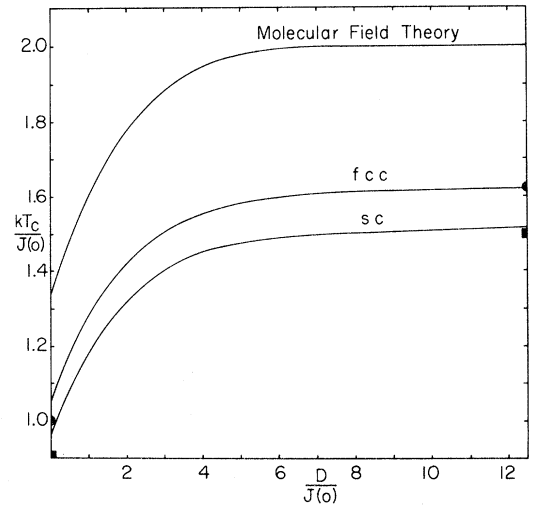

FIG. 8. Plot of Curie temperature $kT_c/J(0)$ vs anisotropy strength $D/J(0)$ for the spin-1 Heisenberg ferromagnet with easy-axis single-ion anisotropy in fcc and sc lattices. High-temperature-expansion values at the limit of $D=0$ (isotropic Heisenberg) and $D=\infty$ (Ising $\frac{1}{2}$) are given in circular (fcc) and square (sc) dots, respectively.

Along with Dyson's correction, the single-ion anisotropy gives a series of terms. The leading-order term of the series is proportional to $T^2e^{-\beta D}$ with a factor depending on the anisotropy strength. Comparing this anisotropy term with the Dyson's correction in the weak-anisotropy limit, we note that, for temperatures less than $\frac{1}{10}$ of the Curie temperature, the anisotropy term dominates even for D as small as $\frac{1}{100}$ of $J(0)$.

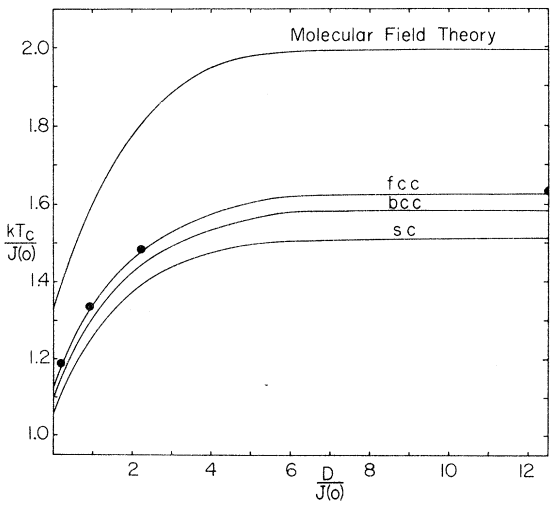

FIG. 9. Plot of Curie temperature vs anisotropy strength for spin-1 Ising ferromagnet with easy-axis single-ion anisotropy, in sc, bcc, and fcc lattices. High-temperature-expansion values for the fcc lattice are shown in dots.

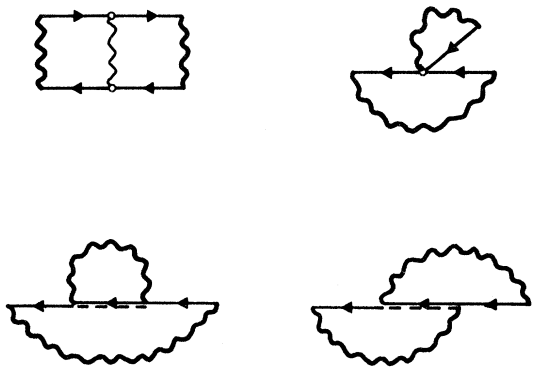

FIG. 10. Free-energy diagrams for the calculation of second-order corrections to $\langle S^z\rangle$ at low temperatures.

Similarly, the second-order correction to the thermal average of $(S^z)^2 = L_{11} + L_{\bar{1}\bar{1}}$ can be obtained. We have

$$\delta^{(2)}\langle (S^z)^2\rangle = \delta^{(2)}\langle S^z\rangle + \frac{1}{N^2}\sum_{k,q}\frac{[J(k)+J(q)]^2}{[D-J(k)-J(q)]^2}n(\omega_k^-)n(\omega_q^-) .$$

The low-temperature expansion gives

$$\delta^{(2)}\langle (S^z)^2\rangle = \delta^{(2)}\langle S^z\rangle + \frac{[2J(0)]^2}{[D-2J(0)]^2}Z_{3/2}^2(D+g\mu_B H)\tau^3+\cdots .$$

In the isotropic case, the leading-order correction due to the spin-wave–spin-wave interactions is proportional to τ^3, while for an anisotropic ferromagnet, a τ^2 term as that given in Eq. (5.24) emerges.

VI. SUMMARY

We have applied the Green's-function diagrammatic technique developed in I to a spin-1 Heisenberg ferromagnet with an easy-axis single-ion anisotropy. Diagrams are classified according to the number of free-momentum variables in the diagrams; i.e., an nth-order diagram has n free-momentum variables summed over in the calculation of its contribution. We have shown that the inconsistency (or redundancy) occurring in the Green's-function theories using the RPA decoupling technique does not arise in our calculation, in which diagrams are summed consistently according to the above classification. As a further support of our theory, we have shown that the Curie temperatures of our calculation agree, within a few percent (1% for the Ising limit), to the values obtained by the high-temperature-expansion technique, and that

the low-temperature behavior of the magnetization reduces to Dyson's results to the first Born approximation, in the isotropic limit. We conclude that we have obtained a self-consistent theory which describes the anisotropic ferromagnet for the whole range of temperature.

ACKNOWLEDGMENT

We would like to thank Dr. Robert A. Kromhout for comments concerning the manuscript, Dr. T. Morita and Dr. T. Horiguchi for sending us a table of the lattice Green's function for the cubic lattices.

---

*Supported by NSF under Grant No. GH-40174.

[1]M. E. Lines, Phys. Rev. 156, 534 (1967).

[2]T. Murao and T. Matsubara, J. Phys. Soc. Jpn. 25, 352 (1968).

[3]J. F. Devlin, Phys. Rev. B 4, 136 (1971).

[4]M. Tanaka and Y. Kondo, Prog. Theor. Phys. 48, 1815 (1972).

[5]N. A. Potapkov, Teor. Mat. Fiz. 8, 381 (1971).

[6]S. B. Haley and P. Erdös, Phys. Rev. B 5, 1106 (1972).

[7]J. Hubbard, Proc. R. Soc. A 285, 542 (1965).

[8]C. Vettier, J. Phys. C 7, 3583 (1974).

[9]T. Egami and M. S. S. Brooks (private communication).

[10]V. G. Vaks, A. I. Larkin, and S. A. Pikin, Zh. Eksp. Teor. Fiz. 53, 281 (1967); 53, 1089 (1967) [Sov. Phys.-JETP 26, 188 (1968); 26, 647 (1968)].

[11]R. B. Stinchcombe, J. Phys. C 3, 2266 (1970).

[12]M. Matlak, Acta Phys. Pol. A 43, 475 (1972).

[13]M. Matlak and B. Westwanski, Acta Phys. Pol. A 44, 57 (1973).

[14]M. P. Kashchenko, N. F. Balakhonov, and L. V. Kurbatov, Zh. Eksp. Teor. Fiz. 64, 391 (1973) [Sov. Phys.-JETP 37, 201 (1973)].

[15]D. H.-Y. Yang and Y.-L. Wang, Phys. Rev. B 10, 4714 (1974).

[16]H. B. Callen, in *Physics of Many-Particle Systems*, edited by E. Meeron (Gordon and Breach, New York, 1966), Vol. 1, Chap. 3, p. 183.

[17]See L. P. Kadanoff and G. Baym, in *Quantum Statistical Mechanics*, edited by D. Pines (Benjamin, New York, 1962), Appendix, p. 196.

[18]G. S. Rushbrooke and P. J. Wood, J. Mol. Phys. 1, 257 (1958); J. Gammel, W. Marshall, and L. Morgan, Proc. R. Soc. A 275, 257 (1963).

[19]See L. J. de Jongh and A. R. Miedema, Adv. Phys. 23, 135 (1974), and reference therein; see also C. Domb, Adv. Phys. 19, 339 (1970); M. E. Fisher, Rep. Prog. Phys. 30, 615 (1967).

[20]See C. Domb and A. R. Miedema, in *Progress in Low Temperature Physics*, edited by C. J. Gorter (North-Holland, Amsterdam, 1964), Vol. IV, Chap. 4; also review papers in Ref. 19. The sc and bcc values are estimated from the figures in the second paper of Ref. 21.

[21]J. Oitmaa, J. Phys. C 5, 435 (1972); J. G. Brankov, J. Pryzstawa, and E. Praveczki, J. Phys. C 5, 3387 (1972); D. M. Saul, Michael Wortis, and D. Stauffer, Phys. Rev. B 9, 4964 (1974).

[22]The values of the coefficients α, C_1, and C_2 are, respectively, $\frac{1}{6}a^2$, 0, $-\frac{1}{12}a^2$ for sc lattice; $\frac{1}{8}a^2$, $-\frac{1}{16}a^2$, $\frac{1}{24}a^2$ for bcc lattice; and $\frac{1}{12}a^2$, $-\frac{1}{32}a^2$, $\frac{1}{96}a^2$ for fcc lattice. The lattice parameter a is taken as 1 for sc, $2^{1/3}$ for bcc, and $2^{2/3}$ for fcc.

[23]F. J. Dyson, Phys. Rev. 102, 1217 (1956); 102, 1230 (1956).